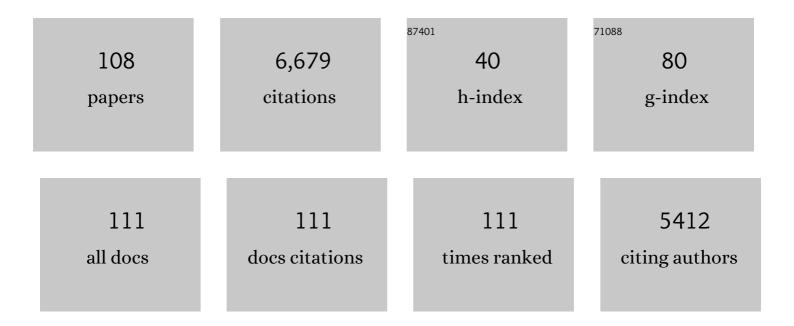
List of Publications by Year in descending order

Source: https://exaly.com/author-pdf/3396295/publications.pdf Version: 2024-02-01



#	Article	IF	CITATIONS
1	Enhanced visibility through microbubble-induced photoacoustic fluctuation imaging. JASA Express Letters, 2022, 2, 012001.	0.5	1
2	Effect of Thermal History and Hydrocarbon Core Size on Perfluorocarbon Endoskeletal Droplet Vaporization. Langmuir, 2022, 38, 2634-2641.	1.6	2
3	Acoustically manipulating internal structure of disk-in-sphere endoskeletal droplets. Nature Communications, 2022, 13, 987.	5.8	12
4	Microbubble Size and Dose Effects on Pharmacokinetics. ACS Biomaterials Science and Engineering, 2022, 8, 1686-1695.	2.6	17
5	Nanobubbles are Non-Echogenic for Fundamental-Mode Contrast-Enhanced Ultrasound Imaging. Bioconjugate Chemistry, 2022, 33, 1106-1113.	1.8	6
6	Ultrasound Contrast Agents. , 2021, , 639-653.		3
7	Contrast-Enhanced Sonography with Biomimetic Lung Surfactant Nanodrops. Langmuir, 2021, 37, 2386-2396.	1.6	1
8	Photoacoustic Impulse Response of Lipid-Coated Ultrasound Contrast Agents. IEEE Transactions on Ultrasonics, Ferroelectrics, and Frequency Control, 2021, 68, 2311-2314.	1.7	2
9	Microbubbles and Nanodrops for photoacoustic tomography. Current Opinion in Colloid and Interface Science, 2021, 55, 101464.	3.4	10
10	Detecting insulitis in type 1 diabetes with ultrasound phase-change contrast agents. Proceedings of the United States of America, 2021, 118, .	3.3	3
11	Treatment of a Rat Model of LPS-Induced ARDS via Peritoneal Perfusion of Oxygen Microbubbles. Journal of Surgical Research, 2020, 246, 450-456.	0.8	17
12	Simulation of xâ€rayâ€induced acoustic imaging for absolute dosimetry: Accuracy of image reconstruction methods. Medical Physics, 2020, 47, 1280-1290.	1.6	18
13	Acoustic nanodrops for biomedical applications. Current Opinion in Colloid and Interface Science, 2020, 50, 101383.	3.4	14
14	Perfusion-guided sonopermeation of neuroblastoma: a novel strategy for monitoring and predicting liposomal doxorubicin uptake <i>in vivo</i> . Theranostics, 2020, 10, 8143-8161.	4.6	17
15	The effect of size range on ultrasound-induced translations in microbubble populations. Journal of the Acoustical Society of America, 2020, 147, 3236-3247.	0.5	12
16	Microbubble Agents: New Directions. Ultrasound in Medicine and Biology, 2020, 46, 1326-1343.	0.7	118
17	Phospholipid Oxygen Microbubbles for Image-Guided Therapy. Nanotheranostics, 2020, 4, 83-90.	2.7	20
18	Changes in microbubble dynamics upon adhesion to a solid surface. Applied Physics Letters, 2020, 116, 123703.	1.5	3

#	Article	IF	CITATIONS
19	Bubble Inflation Using Phase-Change Perfluorocarbon Nanodroplets as a Strategy for Enhanced Ultrasound Imaging and Therapy. Langmuir, 2020, 36, 2954-2965.	1.6	20
20	Vaporizable endoskeletal droplets via tunable interfacial melting transitions. Science Advances, 2020, 6, eaaz7188.	4.7	16
21	Microbubble Radiation Force-Induced Translation in Plane-Wave Versus Focused Transmission Modes. IEEE Transactions on Ultrasonics, Ferroelectrics, and Frequency Control, 2019, 66, 1856-1865.	1.7	9
22	Effect of Hydrostatic Pressure, Boundary Constraints and Viscosity on the Vaporization Threshold of Low-Boiling-Point Phase-Change Contrast Agents. Ultrasound in Medicine and Biology, 2019, 45, 968-979.	0.7	19
23	Ultrasound-mediated delivery of siESE complexed with microbubbles attenuates HER2+/- cell line proliferation and tumor growth in rodent models of breast cancer. Nanotheranostics, 2019, 3, 212-222.	2.7	15
24	Pre-clinical assessment of a water-in-fluorocarbon emulsion for the treatment of pulmonary vascular diseases. Drug Delivery, 2019, 26, 147-157.	2.5	6
25	Designing Oxygen Microbubbles for Treating Tumor Hypoxia. , 2019, , .		1
26	Single Microbubble Measurements for Bound and Unbound Conditions. , 2019, , .		0
27	Ultrasound radiation force as a method to characterize the viscosity of microbubble shells. , 2019, , .		0
28	Perfusion-Guided Monitoring of Tumor Response to Sonoporation and Prediction of Liposomal Doxorubicin Uptake Using Microbubble Contrast Agents. , 2019, , .		0
29	Single Microbubble Measurements for Bound and Unbound Conditions. , 2019, , .		О
30	Intermolecular Forces Model for Lipid Microbubble Shells. Langmuir, 2019, 35, 10042-10051.	1.6	16
31	Click Conjugation of Cloaked Peptide Ligands to Microbubbles. Bioconjugate Chemistry, 2018, 29, 1534-1543.	1.8	31
32	Photoacoustic technique to measure temperature effects on microbubble viscoelastic properties. Applied Physics Letters, 2018, 112, 111905.	1.5	23
33	A Study of Radiation Force Effects in Plane-Wave Transmission Mode. , 2018, , .		1
34	Reverse engineering the ultrasound contrast agent. Advances in Colloid and Interface Science, 2018, 262, 39-49.	7.0	41
35	State-of-the-art of microbubble-assisted blood-brain barrier disruption. Theranostics, 2018, 8, 4393-4408.	4.6	113
36	Plane-Wave Contrast Imaging: A Radiation Force Point of View. IEEE Transactions on Ultrasonics, Ferroelectrics, and Frequency Control, 2018, 65, 2296-2300.	1.7	9

#	Article	IF	CITATIONS
37	Preâ€clinical application of aerosolized waterâ€inâ€fluorocarbon emulsion intrapulmonary drug delivery system for targeting pulmonary vascular diseases. FASEB Journal, 2018, 32, 858.1.	0.2	0
38	Hydrostatic Pressurization of Lung Surfactant Microbubbles: Observation of a Strain-Rate Dependent Elasticity. Langmuir, 2017, 33, 13699-13707.	1.6	10
39	Methods of Generating Submicrometer Phase-Shift Perfluorocarbon Droplets for Applications in Medical Ultrasonography. IEEE Transactions on Ultrasonics, Ferroelectrics, and Frequency Control, 2017, 64, 252-263.	1.7	62
40	Single microbubble measurements of temperature dependent viscoelastic properties. , 2017, , .		0
41	Notice of Removal: Daily intra-tumoral administration of oxygen microbubbles slows tumor growth in the absence of other therapy in a rat subcutaneous fibrosarcoma model. , 2017, , .		0
42	Notice of Removal: Oxygen microbubbles improve tumor control after radiotherapy in a rat fibrosarcoma model. , 2017, , .		1
43	Microbubble gas volume: A unifying dose parameter in blood-brain barrier opening by focused ultrasound. Theranostics, 2017, 7, 144-152.	4.6	79
44	Notice of Removal: Tumor hypoxia modulation dynamics using intra-tumoral, intra-peritoneal and intra-venous oxygen microbubbles administrations — In vivo real-time measurements via spectroscopic absorbance on a rat subcutaneous fibrosarcoma model. , 2017, , .		0
45	Single microbubble measurements of temperature dependent viscoelastic properties. , 2017, , .		0
46	Peritoneal Membrane Oxygenation Therapy for Rats With Acute Respiratory Distress Syndrome1. Journal of Medical Devices, Transactions of the ASME, 2016, 10, 020905.	0.4	4
47	Stability of Monodisperse Phospholipid-Coated Microbubbles Formed by Flow-Focusing at High Production Rates. Langmuir, 2016, 32, 3937-3944.	1.6	74
48	On the thermodynamics and kinetics of superheated fluorocarbon phase-change agents. Advances in Colloid and Interface Science, 2016, 237, 15-27.	7.0	56
49	Single Microbubble Measurements of Lipid Monolayer Viscoelastic Properties for Small-Amplitude Oscillations. Langmuir, 2016, 32, 9410-9417.	1.6	42
50	Microbubble lipid shell elasticity: Simulation and measurement. , 2016, , .		1
51	Combined sonodynamic and antimetabolite therapy for the improved treatment of pancreatic cancer using oxygen loaded microbubbles as a delivery vehicle. Biomaterials, 2016, 80, 20-32.	5.7	116
52	Application of Elastography for the Noninvasive Assessment of Biomechanics in Engineered Biomaterials and Tissues. Annals of Biomedical Engineering, 2016, 44, 705-724.	1.3	27
53	Reducing Tumour Hypoxia via Oral Administration of Oxygen Nanobubbles. PLoS ONE, 2016, 11, e0168088.	1.1	52
54	Design and Development of a Rat Peritoneal Infusion Device for Oxygen Microbubble Bolus Delivery1. Journal of Medical Devices, Transactions of the ASME, 2016, 10, .	0.4	0

#	Article	IF	CITATIONS
55	High Efficiency Molecular Delivery with Sequential Low-Energy Sonoporation Bursts. Theranostics, 2015, 5, 1419-1427.	4.6	25
56	Therapeutic gas delivery via microbubbles and liposomes. Journal of Controlled Release, 2015, 209, 139-149.	4.8	100
57	Ultrasound-modulated fluorescence based on donor-acceptor-labeled microbubbles. Journal of Biomedical Optics, 2015, 20, 036012.	1.4	6
58	Thermal Activation of Superheated Lipid-Coated Perfluorocarbon Drops. Langmuir, 2015, 31, 4627-4634.	1.6	63
59	Fluorocarbon Nanodrops as Acoustic Temperature Probes. Langmuir, 2015, 31, 10656-10663.	1.6	26
60	The Treatment of Acute Respiratory Distress Syndrome in Rats With a Peritoneal Dosing System1. Journal of Medical Devices, Transactions of the ASME, 2015, 9, 020929.	0.4	1
61	Optically induced resonance of nanoparticle-loaded microbubbles. Optics Letters, 2014, 39, 3732.	1.7	21
62	Engineering optically triggered droplets for photoacoustic imaging and therapy. Biomedical Optics Express, 2014, 5, 4417.	1.5	49
63	Microbubble dispersions of natural lung surfactant. Current Opinion in Colloid and Interface Science, 2014, 19, 480-489.	3.4	11
64	Ultrasound-modulated fluorescence based on fluorescent microbubbles. Journal of Biomedical Optics, 2014, 19, 085005.	1.4	19
65	Systemic oxygen delivery by peritoneal perfusion of oxygen microbubbles. Biomaterials, 2014, 35, 2600-2606.	5.7	59
66	State-of-the-art materials for ultrasound-triggered drug delivery. Advanced Drug Delivery Reviews, 2014, 72, 3-14.	6.6	376
67	Better contrast with vesicles. Nature Nanotechnology, 2014, 9, 248-249.	15.6	10
68	Condensation Phase Diagrams for Lipid-Coated Perfluorobutane Microbubbles. Langmuir, 2014, 30, 6209-6218.	1.6	36
69	Single-Particle Optical Sizing of Microbubbles. Ultrasound in Medicine and Biology, 2014, 40, 138-147.	0.7	27
70	Peritoneal Microbubble Oxygenation: An Extrapulmonary Respiration Treatment in Rabbits1. Journal of Medical Devices, Transactions of the ASME, 2014, 8, .	0.4	3
71	Enhanced photoacoustic response with plasmonic nanoparticle-templated microbubbles. Soft Matter, 2013, 9, 7743.	1.2	45
72	The effect of lipid monolayer in-plane rigidity on inÂvivo microbubble circulation persistence. Biomaterials, 2013, 34, 6862-6870.	5.7	93

5

#	Article	IF	CITATIONS
73	In Vivo Demonstration of Cancer Molecular Imaging with Ultrasound Radiation Force and Buried-Ligand Microbubbles. Molecular Imaging, 2013, 12, 7290.2013.00052.	0.7	27
74	Lung Surfactant Microbubbles Increase Lipophilic Drug Payload for Ultrasound-Targeted Delivery. Theranostics, 2013, 3, 409-419.	4.6	43
75	In vivo demonstration of cancer molecular imaging with ultrasound radiation force and buried-ligand microbubbles. Molecular Imaging, 2013, 12, 357-63.	0.7	12
76	Lipid monolayer collapse and microbubble stability. Advances in Colloid and Interface Science, 2012, 183-184, 82-99.	7.0	115
77	Effect of Surface Architecture on InÂVivo Ultrasound Contrast Persistence of Targeted Size-Selected Microbubbles. Ultrasound in Medicine and Biology, 2012, 38, 492-503.	0.7	34
78	Lipid monolayer dilatational mechanics during microbubble gas exchange. Soft Matter, 2012, 8, 4756.	1.2	53
79	Oxygen Gas–Filled Microparticles Provide Intravenous Oxygen Delivery. Science Translational Medicine, 2012, 4, 140ra88.	5.8	95
80	Polyplex-microbubble hybrids for ultrasound-guided plasmid DNA delivery to solid tumors. Journal of Controlled Release, 2012, 157, 224-234.	4.8	112
81	The role of poly(ethylene glycol) brush architecture in complement activation on targeted microbubble surfaces. Biomaterials, 2011, 32, 6579-6587.	5.7	68
82	Microbubble-Size Dependence of Focused Ultrasound-Induced Blood–Brain Barrier Opening in Mice <i>In Vivo</i> . IEEE Transactions on Biomedical Engineering, 2010, 57, 145-154.	2.5	217
83	Effect of Microbubble Size on Fundamental Mode High Frequency Ultrasound Imaging in Mice. Ultrasound in Medicine and Biology, 2010, 36, 935-948.	0.7	156
84	INJECTABLE OXYGEN DELIVERY BASED ON PROTEIN-SHELLED MICROBUBBLES. Nano LIFE, 2010, 01, 215-218.	0.6	22
85	Microbubble Dissolution in a Multigas Environment. Langmuir, 2010, 26, 6542-6548.	1.6	132
86	Phospholipid-Stabilized Microbubble Foam for Injectable Oxygen Delivery. Langmuir, 2010, 26, 15726-15729.	1.6	80
87	Ligand Conjugation to Bimodal Poly(ethylene glycol) Brush Layers on Microbubbles. Langmuir, 2010, 26, 13183-13194.	1.6	56
88	Microbubble shell break-up and collapse during gas exchange. , 2010, , .		2
89	Comparing tumor response to VEGF blockade therapy using high frequency ultrasound imaging with size-selected microbubble contrast agents. , 2010, , .		0
90	Microbubble compositions, properties and biomedical applications. Bubble Science, Engineering & Technology, 2009, 1, 3-17.	0.2	444

#	Article	IF	CITATIONS
91	High-frequency ultrasound imaging of size-isolated microbubbles in mice. , 2009, , .		2
92	An in-vivo evaluation of the effects of anesthesia carrier gases on ultrasound contrast agent circulation. , 2009, , .		1
93	The Dependence of the Ultrasound-Induced Blood-Brain Barrier Opening Characteristics on Microbubble Size In Vivo. , 2009, , .		3
94	Microbubble size isolation by differential centrifugation. Journal of Colloid and Interface Science, 2009, 329, 316-324.	5.0	366
95	Nanostructural features on stable microbubbles. Soft Matter, 2009, 5, 716-720.	1.2	24
96	Lung surfactant microbubbles. Soft Matter, 2009, 5, 4835.	1.2	18
97	A stimulus-responsive contrast agent for ultrasound molecular imaging. Biomaterials, 2008, 29, 597-606.	5.7	103
98	DNA and Polylysine Adsorption and Multilayer Construction onto Cationic Lipid-Coated Microbubbles. Langmuir, 2007, 23, 9401-9408.	1.6	127
99	Ultrasound Microbubble Contrast Agents: Fundamentals and Application to Gene and Drug Delivery. Annual Review of Biomedical Engineering, 2007, 9, 415-447.	5.7	1,089
100	Lateral Phase Separation in Lipid-Coated Microbubbles. Langmuir, 2006, 22, 4291-4297.	1.6	119
101	Ultrasound Radiation Force Modulates Ligand Availability on Targeted Contrast Agents. Molecular Imaging, 2006, 5, 7290.2006.00016.	0.7	74
102	Ultrasound radiation force enables targeted deposition of model drug carriers loaded on microbubbles. Journal of Controlled Release, 2006, 111, 128-134.	4.8	253
103	Effect of Microstructure on Molecular Oxygen Permeation through Condensed Phospholipid Monolayers. Journal of the American Chemical Society, 2005, 127, 6524-6525.	6.6	56
104	Surface phase behavior and microstructure of lipid/PEG-emulsifier monolayer-coated microbubbles. Colloids and Surfaces B: Biointerfaces, 2004, 35, 209-223.	2.5	121
105	Oxygen Permeability of Fully Condensed Lipid Monolayers. Journal of Physical Chemistry B, 2004, 108, 6009-6016.	1.2	73
106	Radiation-Force Assisted Targeting Facilitates Ultrasonic Molecular Imaging. Molecular Imaging, 2004, 3, 153535002004041.	0.7	34
107	Radiation-Force Assisted Targeting Facilitates Ultrasonic Molecular Imaging. Molecular Imaging, 2004, 3, 135-148.	0.7	159
108	Dissolution Behavior of Lipid Monolayer-Coated, Air-Filled Microbubbles:Â Effect of Lipid Hydrophobic Chain Length. Langmuir, 2002, 18, 9225-9233.	1.6	298